

DETERMINATION OF ICE DEPOSIT SHAPE AND ICE ACCRETION RATE ON AIRFOIL IN ATMOSPHERIC ICING CONDITIONS AND ITS EFFECTS ON AIRFOIL CHARACTERISTICS

Janusz Sznajder, Adam Sieradzki,
Wieńczysław Stalewski

*Institute of Aviation, Department of Aerodynamics
Krakowska Av. 110/114, 02-256 Warsaw, Poland
tel.: +48 22 8460011 ext. 492, fax: +48 22 8464432
e-mail: janusz.sznajder@ilot.edu.pl, adam.sieradzki@ilot.edu.pl
wienzczyslaw.stalewski@ilot.edu.pl*

Abstract

Simulations of ice accretion on airfoil in icing conditions were conducted using ice accretion model implemented by authors in ANSYS FLUENT CFD solver. The computational model includes several sub-models intended for simulations of two-phase flow, determination of zones of water droplets impinging on the investigated surface, flow of water in a thin film on airfoil surface and heat balance in air-water-ice contact zone. The method operates in an iterative loop, which enables determination of effects of gradual deformation of aircraft surface on airflow over the surface, which has impact on distribution of collected water, flow of water film over the surface and local freezing rates. The implementation of the method in CFD solver made it necessary to complement the mathematical model of determination of local rates of deformation of aircraft surface with modification of computational mesh around the surface, which must conform, to the deformed surface. Results of simulated ice accretion on NACA 0012 airfoil were compared with results of experiment conducted in icing wind tunnel for a 420 s long process of ice accretion in steady-flow, steady angle-of-attack conditions. Close agreement of values and location of maximum ice thickness obtained in experiment and in the flow, simulations can be observed. For the airfoil deformed with ice, contour determination of its aerodynamic characteristics at several other angles of attack was conducted proving dramatic degradation of its aerodynamic characteristics due to ice deformation.

Keywords: aerodynamics, two-phase flow, simulations of ice accretion, Aircraft Engineering, Transport, Vehicles

1. Introduction

Atmospheric conditions allowing for accretion of ice deposits on aircraft surface are frequent in climate existing over most of Europe during more than half a year. The conditions conducive to most intensive icing are characterised by moderate sub-freezing temperatures at which supercooled water droplets hover in clouds. Dispersion data of the supercooled water droplets is collected for different atmospheric temperatures and types of clouds and introduced into flight regulations as basis for design of anti-icing installations. Example of such data is presented in Fig. 1 for stratiform and cumuliform clouds at different temperatures. For aircraft designed for operation in all-weather conditions experimental investigations of operation of most critical components exposed to icing (leading edges of wings and control surfaces, engine inlets, Pitot tubes) are conducted in icing wind tunnels where such conditions are recreated. Apart from experimental investigations, computational simulations of ice accretion on aerodynamic surfaces have important role in aircraft design as they are capable of prediction of progression of ice accretion in time and at the same time of prediction of degradation of aircraft aerodynamic characteristics due to ice accretion at relatively low cost. This capability is important especially because of appearance in recent years of a new class of flying objects – the unmanned drones, which, due to their small size and low installed power are not equipped with anti-icing installations. Such objects may be

exposed to icing conditions because of unexpected degradation of weather conditions and the knowledge of rate of degradation of aerodynamic characteristics in case of encountering icing conditions may be critical for their safety.

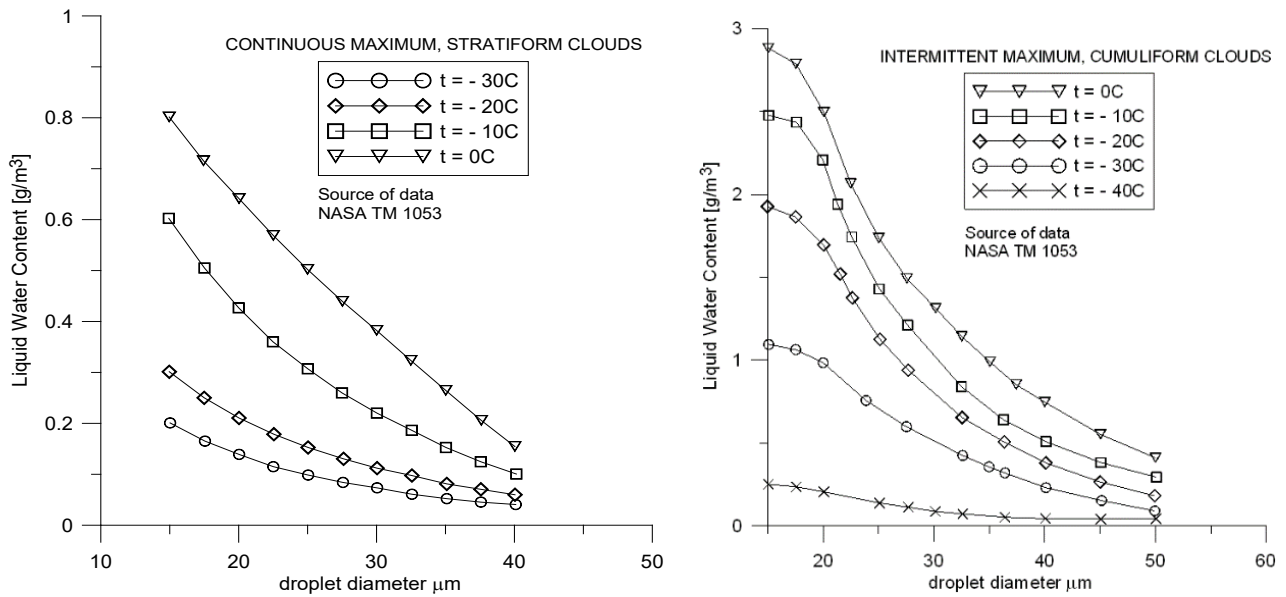


Fig. 1. Dispersion data of supercooled droplets in conditions of atmospheric icing [1]

Simulation of progression of ice accretion on aircraft surface in time involves finding a solution to different problems contributing to the phenomenon. These problems include:

- analysis of two-phase flow problem, consisting of air and dispersed water with the purpose of determination of zones where water hits the surface and surface distribution of mass of water hitting the surface,
- determination of local icing conditions on aerodynamic surface, which may involve rime icing (water hitting the surface freezes instantaneously), or glaze icing (some of the water freezes, remaining fraction flows over the surface). Depending on atmospheric conditions and progression of the phenomenon in time either form of icing, or both, on different parts of the surface are possible,
- modelling of flow of unfrozen water in the water film,
- determination of local freezing rate in each freezing zone (rime and glaze) and of the instantaneous shape of the surface with ice deposit.

Solution of the problems mentioned above must be conducted iteratively in a time loop. Deformation of the surface due to ice accretion changes distribution of mass of water hitting the surface and growing ice thickness may lead to change of the icing form from rime to glaze [2, 3]. It must be noted that the second form, the glaze icing is much more dangerous to the flying object than first one and leads to deformations significantly changing its shape, while the first form produces relatively smooth deformations.

In the presented approach, the solutions to problems contributing to icing phenomenon presented above are implemented in the form of modules of user-defined functions implemented in a general-purpose flow simulation code ANSYS Fluent that enables the solution of the compound problem in an iterative loop in time. The first sub-problem, the solution of two-phase flow problem and determination of mass distribution of water hitting the surface was described in [6] and [7]. The solution for two-phase flow problem was based on modelling the flow of dispersed water in Eulerian approach, as continuous fraction, where the main forces responsible for movement of droplets were droplet drag, gravity and buoyancy. In this article, solutions to the remaining problems are presented.

2. Description of the implemented method of simulation of ice accretion in atmospheric icing conditions

The modelling of ice accretion on aircraft surface dates back to mid-20-th century when model of Messinger [2] was developed, which was the basis of many simulation methods in which different flow simulation methods were used for determination of mass distribution of water hitting the surface. The freezing model of Messinger was based on energy balance including terms describing energy transported into the contact zone (latent heat of freezing droplets, heating in boundary layer, kinetic energy of droplets) and transported away from the surface (convection into air, warming of supercooled droplets, evaporation of water). The limitations of the Messinger model stemmed from its inability to switch from rime icing to glaze icing, with continuously decreasing freezing fraction, and from omitting of conduction of heat through ice layer to the substrate (e.g. wing surface), which under predicted the freezing fraction [3]. In the presented work, the extension of the Messinger model by Myers [3] was implemented in which these problems were corrected.

The implemented model has the following terms representing energy transport, presented below using original notation of work [3]:

a) terms describing energy transported into air-water-ice contact zone:

$$Q_k = (\beta \rho_{d \text{ inf}} V_{\text{inf}}) \frac{v_{\text{inf}}^2}{2} - \text{kinetic energy of water droplets,} \quad (1)$$

$$Q_l = L_f \dot{m}_{\text{ice}} - \text{latent heat of freezing,} \quad (2)$$

$$Q_{ai} = r \cdot \frac{H_{ai} v_{\text{inf}}^2}{2c_a} - \text{heating of ice in the boundary layer,} \quad (3)$$

$$Q_{aw} = r \cdot \frac{H_{aw} v_{\text{inf}}^2}{2c_a} - \text{heat released in the boundary layer,} \quad (4)$$

where r is recovery factor.

b) terms describing energy transported away from the contact zone:

$$Q_c = H_{aw}(T_w - T_a) = q_c(T_w - T_a) - \text{convection over water layer,} \quad (5)$$

$$Q_{ci} = H_{ai}(T_i - T_a) = q_{ci}(T_w - T_a) - \text{convection over ice layer (in rime icing),} \quad (6)$$

$$Q_e = \chi_e e_0(T_w - T_a) = q_e(T_w - T_a) - \text{evaporation heat,} \quad (7)$$

$$Q_s = \chi_s e_0(T_i - T_a) = q_s(T_w - T_a) - \text{sublimation heat,} \quad (8)$$

$$Q_d = \beta \rho_{d \text{ inf}} V_{\text{inf}}(T_w - T_a) = q_d(T_w - T_a) - \text{warming of supercooled droplets,} \quad (9)$$

$$Q_{\text{cond}} = \kappa_i \frac{T_f - T_s}{B} - \text{conduction of heat through ice to substrate,} \quad (10)$$

where H is convection coefficient, used with subscripts denoting target and source of heat flow: a – air, w – water, i – ice.

The growth of rime ice thickness in time is described by equation (11):

$$B = \left(\frac{\beta \rho_{d \text{ inf}} V_{\text{inf}}}{\rho_r} - \dot{m}_s \right) t, \quad (11)$$

where:

\dot{m}_s – mass of sublimating ice in unit time, determined from equation:

$$L_s \dot{m}_s = \chi_s e_0(T - T_a), \quad (12)$$

β – water collection efficiency [5]:

$$\beta = \frac{\rho_d \vec{v}_d \cdot \vec{n}}{\rho_{d \text{ inf}} \cdot \vec{v}_{\text{inf}}}, \quad (13)$$

ρ_a – air density,

ρ_d – density of the dispersed water phase,

ρ_w – water density,

\overline{V}_d – local velocity of the dispersed water phase; subscript “inf” denotes freestream values.

The temperature profile in ice layer is given by:

$$T = T_s + \frac{Q_{ai} + Q_k + \beta \rho_d \inf V_{inf} - (q_{ci} + q_d + q_s)}{\kappa_i + B(q_{ci} + q_d + q_s)} z, \quad (14)$$

where z is distance from the substrate

Growth of rime ice is fully determined by the distribution of mass of water hitting the surface, described by collection efficiency β [3, 4]. In work [3], it was shown that the limit value of ice thickness, beyond which not all captured water freezes upon impact, is given by equation:

$$B_g = \frac{\kappa_i (T_f - T_s)}{\beta \rho_d \inf V_{inf} L_f + [Q_a + Q_k - (q_c + q_d + q_e)(T_f - T_a)]}. \quad (15)$$

Equation (15) may yield positive, negative or infinite values of B_g . Positive value denotes the limiting value of rime ice. Negative value may occur when numerator is negative (surface temperature higher than freezing temperature) or when denominator is negative. This case occurs when there is too little released heat to produce water and the process will only produce rime ice.

In the case when B_g is positive, its value is dependent on local values of terms dependent on mass of captured water and heat transfer so it varies on the surface or along airfoil. Water will first appear in place where B_g is minimum.

The corresponding time is given by:

$$t_g = (\rho_r / \beta \rho_d \inf V_{inf}) B_g. \quad (16)$$

When t_g is exceeded part of the captured water will move along the surface in a thin water film driven mainly by tangential stress produced by the airflow. The water will freeze if in new location the local ice thickness is lower than B_g . So, after exceeding t_g flow simulation must include simulation of water flow in a thin film.

In presence of water, film the rate of ice accretion results from balance of heat transported into and from the ice-water contact zone: [3]:

$$\rho_i L_f \frac{\partial B}{\partial t} = Q_e + Q_d + Q_c - (Q_a + Q_k) + \kappa_i \frac{T_f - T_s}{B}, \quad (17)$$

where the last term describes conduction of heat through ice layer to the substrate.

Modelling of water film flow is based on a method presented in [4]. Water flow in the film is described with two variables: local height δ and local average velocity \bar{u} . The average velocity of water film is evaluated assuming parabolic variation of water velocity with film height.

$$\bar{u} = \frac{\tau \delta}{2\mu} - \frac{\delta^2}{3\mu} \cdot \frac{\partial p}{\partial s} + \frac{1}{2\mu} \delta^2 \vec{g} \cdot \vec{s}. \quad (18)$$

The flow of water takes place with some of the water freezing and evaporating:

$$\frac{\partial \delta}{\partial t} + \text{div}(\bar{u}\delta) = \frac{1}{\rho_w} (V_\infty \beta \rho_d - \dot{m}_e - \dot{m}_{ice}). \quad (19)$$

Mass of freezing water may be determined from equation (16) and mass of evaporating water from equation (19):

$$L_e \dot{m}_e = \chi_e e_0 (T_f - T_a). \quad (20)$$

The core of the implemented method of simulation of ice accretion is discretisation of equations (11), (17) and (19) over the investigated surface (airfoil contour). These equations are integrated numerically in time with a first-order method in a user-defined function module

collecting the necessary data of airflow over the airfoil from the ANSYS Fluent solver. The integration of equations determining flow of water is done separately from integration of airflow equations by the solver. The result is time-dependent distribution of ice accreted over the surface and water film height and average velocity.

An important problem in the implementation of the method of simulation of ice accretion is dependence of the solution of air and dispersed water flow on the computational mesh around the surface. The accreted ice changes the shape of the surface and this change of surface geometry must be transferred to the nodes of the computational mesh surrounding the surface. The ANSYS Fluent solver enables such mesh transformations through the macros in the Dynamic Mesh module, which provide direct access to computational nodes of the mesh. User-defined functions were created which transfer the surface deformation to the computational mesh in the deformable circular zone surrounding the airfoil surface. This deflection of nodes in the deformable zone is gradual, decreasing towards its outer limit with direction gradually changing from normal-to-airfoil surface to normal-to-zone-boundary. In Fig. 2, it is shown how the changes of coordinates of surface points are gradually distributed in the deformable computational zone of airflow including the directions of node movement near the airfoil surface.

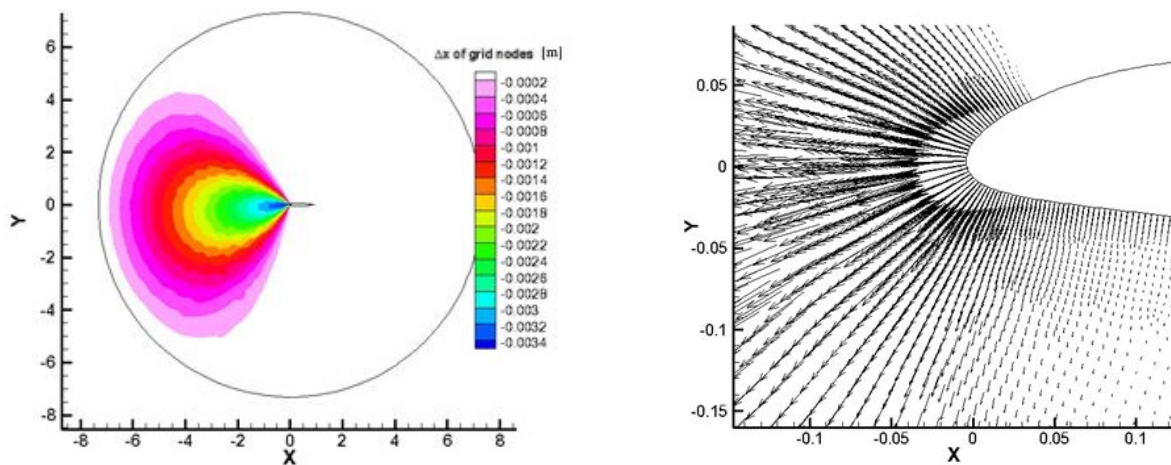


Fig. 2. Transfer of deformation of airfoil surface to nodes of computational mesh in one-step of mesh update. Arrows on the right picture are magnified approximately 100 times

It must be noted, however, that due to irregular shape of icing deformations of the airfoil, that the quality of the modified mesh gradually decreases in time of the simulation. After a number of simulation steps with mesh modified by the user-defined functions, a new high-quality mesh is prepared over the modified surface and the existing air and water flow solution is reinterpolated into a new mesh.

3. Results of icing simulation for NACA 0012 airfoil

Simulation of ice accretion on NACA 0012 airfoil was conducted for conditions of Mach number $Ma = 0.3$, Reynolds number $Re = 4.39$ million, air temperature 262 K (-11°C), dispersed water concentration $\rho_d = 0.55\text{ g/m}^3$, water droplet diameter of $20\text{ }\mu\text{m}$. The results of numerical simulations were compared with results of experiment conducted in icing wind tunnel for the same airfoil and flow conditions. A comparison of ice contours obtained as results of flow simulations using the present method and results of experiment obtained after 420 s of ice accretion [5] is presented in Fig. 3. In Fig. 4 is shown growth in time of ice thickness in the numerical solution. Airflow was modelled using URANS equations with Spalart-Almaras turbulence model with nondimensional y^+ parameter of 30, which is appropriate for this turbulence model and allows for relatively small size of computational mesh. Airflow equations were integrated with time step of

0.003 s and icing equations with time step of 0.01 s. Airfoil contour was updated every 10 s with recalculation of airflow in order to obtain updated values of pressure gradient and distribution of captured mass of water. After half-time of total time of icing simulation the growing deteriorations of computational mesh updated in the flow solver required preparation of a new mesh with mesh editor after every four to five mesh updates in the flow solver.

It can be seen that location and value of maximum thickness of accreted ice is well predicted with the present method and that larger differences between the results of flow simulation and experiment occur near the end of pressure-side zone (lower airfoil surface) of ice accretion than in the centre or at the suction side. The deviations of the computed solution from the results of experiment may be caused by the simplifying assumptions made in modelling the two-phase air and dispersed water flow which include assuming only one droplet diameter and no secondary effects such as droplet deformation near the airfoil surface, break-up of droplets on impact extending the impact zone. It must also be noted that the phenomenon of ice accretion shows spatial variation in the experiment along wingspan at the same free-stream conditions.

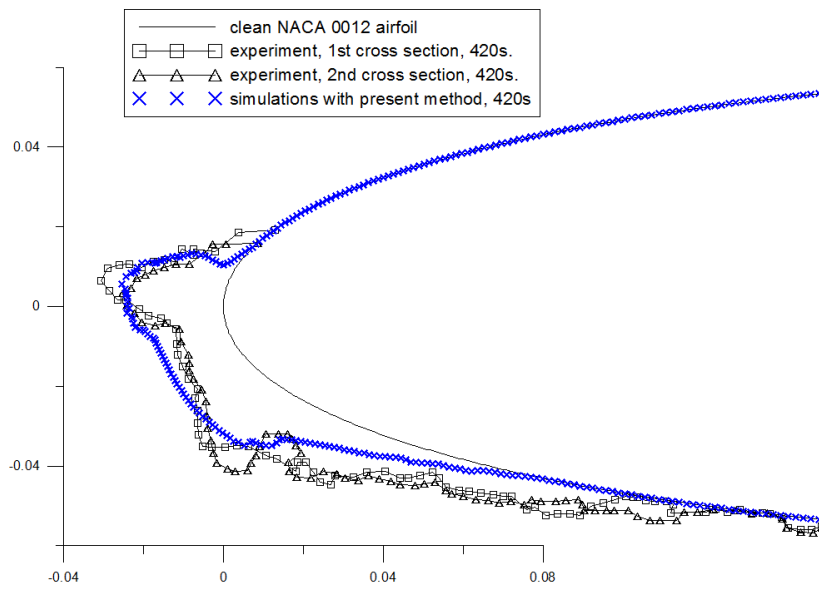


Fig. 3. Comparison of computed airfoil contour with ice and results of experiment in icing wind tunnel after 420 s of ice accretion

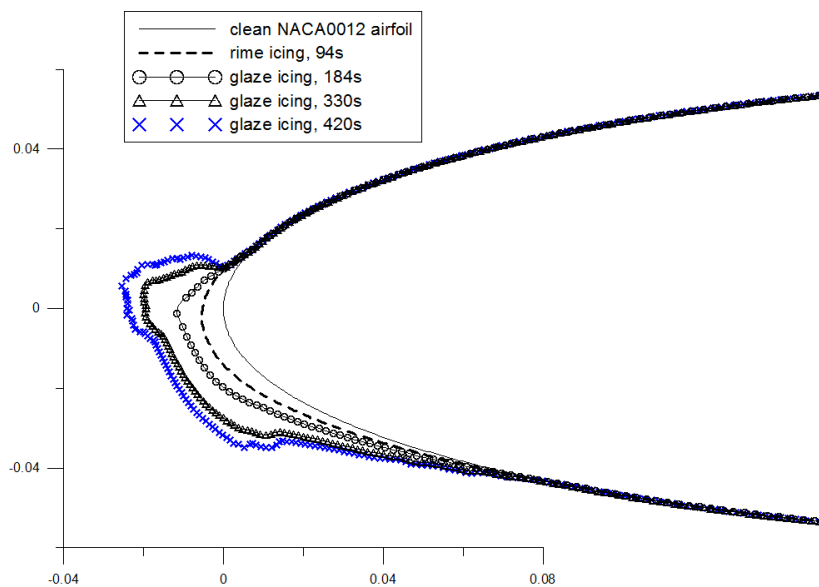


Fig. 4. Growth in time of simulated ice thickness including phases of rime icing and glaze icing

In Fig. 5 and 6 are presented computed lift and drag values of clean NACA 0012 airfoil end of the same airfoil covered with computed ice contour after 420 s long simulated ice accretion. For angle-of-attack, range from approximately 8 degrees onwards starts large reduction of lift, exceeding 50% of available lift of clean airfoil. This reduction of lift takes place with large increase of drag, which achieves values several times higher than clean-airfoil values.

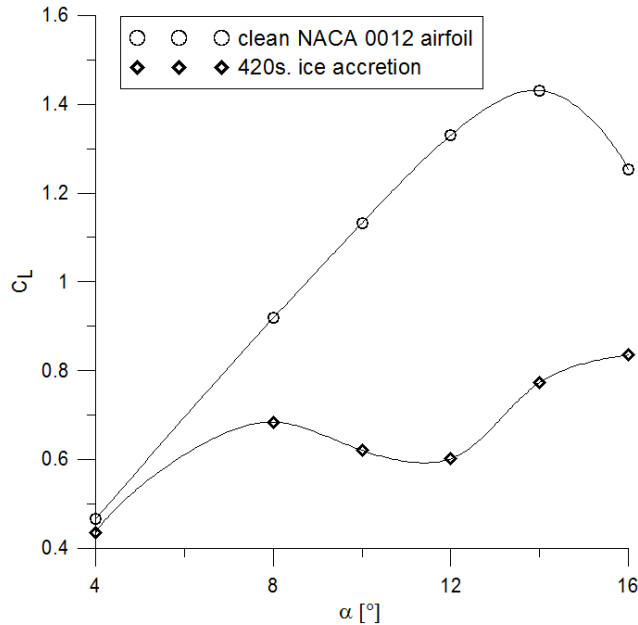


Fig. 5. Comparison of computed lift values vs. angle of attack for clean NACA 0012 airfoil and for the same airfoil with ice contour after simulated 420 s-long ice accretion

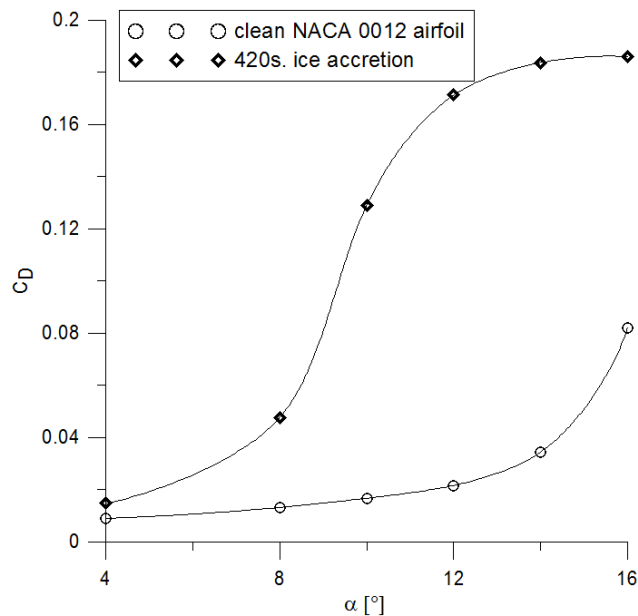


Fig. 6. Comparison of computed drag values vs. angle of attack for clean NACA 0012 airfoil and for the same airfoil with ice contour after simulated 420 s-long ice accretion

4. Conclusions

The presented results of simulation of ice accretion, compared with results of experiment conducted in icing wind tunnel prove ability of the proposed method to predict rate of deformation of airfoil contour in icing conditions and rate of degradation of its aerodynamic characteristics due

to deformation of the airfoil contour due to ice. It can be used to assess impact of ice accretion on aerodynamic characteristics of flying objects, particularly small ones, not equipped with anti-icing installations, by estimation of effects of ice accretion on wings, rotor blades, propellers. The method may be developed further to assess effectiveness of thermal anti-icing installations in prevention of ice accretion on aircraft surface.

References

- [1] Federal Aviation Regulations FAR 25 Appendix C, http://www.flightsimaviation.com/data/FARS/part_25-appC.html.
- [2] Messinger, B. L., *Equilibrium Temperature of an Unheated Icing Surface as a Function of Air Speed*, Journal of the Aeronautical Sciences, Jan., pp. 29-42, 1953.
- [3] Myers, T., *Extension to the Messinger Model for Aircraft Icing*, AIAA Journal, Vol. 39, No. 2, February 2001.
- [4] Morency, F., Brrahimi, M. T., Tezok, F., Paraschivoiu, I., *Hot Air Anti-Icing System Modelization in the Ice Prediction Code Canice*, AIAA-98-0192, American Institute of Aeronautics and Astronautics, Inc., 1997.
- [5] Beaugendre, H., Morency, F., Habashi, W., *Development of a second generation In-Flight Icing Simulation Code*, Journal of Fluids Engineering, Vol. 128 (2), pp. 378-387, 2006.
- [6] Hospers, J. M., Hoeijmakers, H. W. M., *Numerical Simulation of SLD Ice Accretions*, 27th International Congress of the Aeronautical Sciences, 2010.
- [7] Sznajder, J., *Determination of water collection on two- and three-dimensional aerodynamic surfaces in external two-phase flow in atmospheric conditions*, Journal of KONES Powertrain and Transport, Vol. 23, No. 1, pp. 369-376, 2016.